Gradient elasticity and flexural wave dispersion in carbon nanotubes

Harm Askes*
Department of Civil and Structural Engineering, University of Sheffield, Sheffield S1 3JD, United Kingdom

Elias C. Aifantis†
School of Engineering, Laboratory of Mechanics and Materials, Aristotle University of Thessaloniki, 54006 Thessaloniki, Greece and College of Engineering, Center for Mechanics of Materials, Instabilities and Manufacturing Processes, Michigan Technological University, Houghton, Michigan 49931, USA

(Received 25 January 2009; revised manuscript received 24 August 2009; published 17 November 2009)

Higher-order elasticity theories have recently been used to predict the dispersion characteristics of flexural waves in carbon nanotubes (CNTs). In particular, nonlocal elasticity and gradient elasticity (with unstable strain gradients) have been employed within the framework of classical Euler-Bernoulli or improved Timoshenko beam theory to capture the dynamical behavior of CNTs. Qualitative agreement with the predictions of related molecular-dynamics (MD) simulations was observed, whereas the MD results departed significantly from those obtained with classical elasticity calculations. The present contribution aims to alert that the aforementioned higher-order models may yield questionable results for the higher wave numbers. As an alternative, gradient elasticity (with stable strain gradients), by also incorporating inertia gradients for dynamical applications, is used in combination with both Euler-Bernoulli and Timoshenko beam theories and shown to describe flexural wave dispersion in CNTs realistically for the small-to-medium range of wave numbers, i.e., the range for which MD results are available.

DOI: 10.1103/PhysRevB.80.195412 PACS number(s): 62.30.+d

I. INTRODUCTION

The modeling of flexural waves in carbon nanotubes (CNTs) must account, among other phenomena, for the dispersive behavior that is caused by their inherent nanoscale heterogeneity, in accordance with related molecular-dynamics (MD) simulations. Classical elasticity in conjunction with beam and shell theory has been remarkably successful, and in line with MD simulations, to model certain nanoscale stationary and time-dependent configurations.[1,2] However, heterogeneity effects due to a pre-existing or inhomogeneously evolving nanostructure may not be accounted for by classical elasticity and, thus, a modified elasticity theory incorporating nonlocal and/or gradient effects is more appropriate to use.[3–7] In fact, some recent studies have addressed this issue, using certain types of nonlocality or long-range interaction as an extension of the classical equations of elasticity. In particular *gradient elasticity*, where the standard constitutive equations of elasticity are generalized by incorporating the Laplacian of stress and/or strain, has been used to model deformation processes in very small volumes,[8,9] to capture size effects[10,11] and, of particular relevance to the present paper, to describe the dynamic behavior of CNTs.[12–16]

Various formats of gradient elasticity are used in the studies mentioned above. In this paper we review these different formulations and compare their behavior for CNTs in Sec. II, focusing on the stability or otherwise of the various types of gradients used. In Sec. III, beam theories will be formulated based on stable gradient elasticity formulations. We will employ Euler-Bernoulli theory as well as Timoshenko theory, and formulate these beam theories in terms of gradient elasticity with stress gradients as well as gradient elasticity with combined strain/inertia gradients. In Sec. IV we review the work of Wang and Hu on CNTs, who used an unstable variant of gradient elasticity. Even though this theory has been used by several researchers as being directly motivated from atomistic interactions, it does not ensure uniqueness of solution in related boundary-value problems. Its general use should thus be restricted, despite of the fact that dispersive wave propagation results are consistent with lattice dynamics in the Brillouin zone. Nevertheless, the theory can be retrieved from one of the more general theories of Sec. III through a particular parameter choice. An overall comparison of the various gradient elasticity models will be given in Sec. V and the capacity of each model to simulate the dispersion of flexural waves in CNTs will then be verified.

II. GRADIENT ELASTICITY THEORIES RELEVANT FOR WAVE DISPERSION

Starting with the work of Aifantis,[8] higher-order gradient and nonlocal elasticity theories of the type advocated by Mindlin,[17] Kröner,[18] and Eringen[19] have been revisited by adopting simpler and more robust formats for solving boundary-value problems to address, among others, elimination of singularities from crack tips[20–22] and dislocation lines,[23,24] size effects,[9–11] and wave dispersion.[25,26] At first glance, Aifantis' format of gradient elasticity may be obtained from Mindlin's format through a specific choice of parameters, thereby reducing the number of length scale parameters from five to one. However, the physical motivation of this particular choice of parameter reduction was not obvious[27] as other choices for parameter reduction would not lead to similar robust models. Moreover, the two approaches differ in scope and application; Mindlin's approach has been used mainly for wave propagation studies but not for size effects and the elimination of elastic singularities. A simplified version of gradient elasticity accounting for gradient effects of both Mindlin's and Eringen's type has been discussed by Gutkin and Aifantis,[28–31] based on earlier unpublished work by Ru and Aifantis,[32] for static problems by incorporating both stress and strain gradients. It reads as

$$\sigma_{ij} - \ell_1^2 \sigma_{ij,mm} = C_{ijkl}(\varepsilon_{kl} - \ell_2^2 \varepsilon_{kl,mm}) \tag{1}$$

where σ_{ij} and ε_{ij} are stress and strain tensors, C_{ijkl} contains the elastic moduli, while ℓ_1 and ℓ_2 denote internal length scales to be determined by experiment or microscopic models such as MD simulations. As already mentioned, the above form of gradient elasticity is quite sufficient for static problems and it has been successfully tested for eliminating elastic singularities at crack tips and dislocation lines, thus providing estimates for the size of the fracture process zone and dislocation cores.[3,9] When $\ell_1=0$ the theory is a special form of Mindlin's strain gradient elasticity and when $\ell_2=0$ the theory reduces to Eringen's 1983 stress gradient elasticity theory (which itself was obtained from Eringen's earlier integral nonlocal elasticity theory by assuming a particular nonlocal kernel).

A difference between Eringen's 1983 theory and Eq. (1) concerns how the balance of momentum is formulated: Eringen uses the divergence of σ_{ij} whereas Gutkin and Aifantis use the divergence of the right-hand side of Eq. (1). This difference implies an interchange of the roles of stress and strain and it becomes significant in dynamics: Eringen's theory predicts a phase velocity that is monotonically decreasing with the wave number, whereas the phase velocity would be monotonically increasing in the theory of Gutkin and Aifantis. However, the latter theory was formulated for use in statics, and for dynamic applications additional considerations involving inertia gradients need to be considered.[25,26,33,34] Since the present study is concerned with the dynamical behavior of CNTs by using gradient elasticity, the dynamical extension of the aforementioned stress/strain gradient theory is discussed here along somewhat different lines than in the aforementioned papers, and we will link this particular theory of gradient elasticity to other formats that have been proposed to describe dispersive wave propagation, such as[35,36]

$$\sigma_{ij} = C_{ijkl}(\varepsilon_{kl} + \ell^2 \varepsilon_{kl,mm}). \tag{2}$$

The derivation of such models from related discrete models (consisting of masses and springs, e.g.) is straightforward, which simplifies the identification of the internal length scale ℓ. For the small-to-medium range wave numbers improved accuracy of the phase velocity and the angular frequency is obtained. However, beyond a certain cutoff wave number, imaginary phase velocities are found which are destabilizing. Equation (2) was used by Wang and Hu[12] to describe wave dispersion in CNTs.

The unstable strain gradients format of Eq. (2) can be replaced by stable stress gradients format via a simple mathematical manipulation. Multiplying the Laplacian of Eq. (2) with ℓ^2 and subtracting the result from Eq. (2) yields

$$\sigma_{ij} - \ell^2 \sigma_{ij,mm} = C_{ijkl}\varepsilon_{kl} \tag{3}$$

where terms of order $O(\ell^4)$ have been ignored. As already mentioned, this model was first derived from an integral nonlocal model by Eringen,[19] and the corresponding strain energy of this model is positive definite.[37] The model was also used to describe wave dispersion in CNTs.[13–16] A similar manipulation of Eq. (2) can be used to arrive at a gradient elasticity theory with inertia gradients. First, the equation of motion corresponding to Eq. (2) is considered, that is,

$$\rho \ddot{u}_i = C_{ijkl}(u_{k,jl} + \ell^2 u_{k,jlmm}) \tag{4}$$

where ρ is the mass density and u_i denotes displacement. The Laplacian of Eq. (4) is multiplied with ℓ^2 and the result is subtracted from Eq. (4) by which[38,39]

$$\rho(\ddot{u}_i - \ell^2 \ddot{u}_{i,mm}) = C_{ijkl}u_{k,jl}. \tag{5}$$

The kinetic energy of such a model is positive definite, therefore the unstable strain gradients of Eq. (2) are replaced by stable inertia gradients.

In Eq. (2), the length scale ℓ can be related to the interparticle spacing d of an associated discrete model via $\ell^2 = \frac{1}{12}d^2$, as has been used by Wang and Hu for CNTs.[12] By implication, the same relation between ℓ and d holds in Eqs. (3) and (5). For such strictly periodic materials the unit-cell size can also be considered to be the size of the Representative Volume Element (RVE). A generalization of this point of view was given recently by Gitman *et al.*[40] who showed that the relation between the length scale ℓ of gradient elasticity and the RVE size holds for random materials as well. In fact, these authors derived a gradient elasticity formulation for dynamics as

$$\rho(\ddot{u}_i - \ell_m^2 \ddot{u}_{i,mm}) = C_{ijkl}(u_{k,jl} - \ell_s^2 u_{k,jlmm}) \tag{6}$$

where the length scales ℓ_m and ℓ_s are related to inertia gradients and strain gradients, respectively. As indicated above, the strain gradient length scale ℓ_s is related to the RVE size in elastostatics and should for periodic microstructures (such as CNTs) be taken as $\ell_s^2 = \frac{1}{12}d^2$ where d is the unit-cell size. On the other hand, the inertia gradient length scale ℓ_m is related to the RVE size for elastodynamics, which tends to be larger than the RVE size for elastostatics. The inclusion of the additional material parameter ℓ_m allows a more accurate modeling of a wider range of phenomena exhibiting wave dispersion, while MD simulations can be used to provide quantitative estimates for ℓ_m—both suggestions will be demonstrated in Sec. V. The model of Eq. (6) may, again, formally be considered as a special case of Mindlin's theory, although without a clear physical motivation. It has also been derived directly from a discrete model of masses and springs.[25,41]

III. BEAM THEORIES BASED ON GRADIENT ELASTICITY

In this section, we will formulate Euler-Bernoulli beam (EBB) and Timoshenko beam (TB) beam theories combined with stress gradients as well as combined strain/inertia gradients to model dispersion of flexural waves in CNTs. The gradient elasticity formulation with unstable strain gradients can be retrieved from Eq. (6) by setting $\ell_m^2=0$ and $\ell_s^2=-\ell^2$, whereas the formulation with inertia gradients is found from

Eq. (6) by setting $\ell_m^2=\ell^2$ and $\ell_s^2=0$. A related dynamical problem based on these considerations for the free transverse vibrations of double-walled CNTs has also been considered recently.[3]

A. Preliminaries

The formulation of gradient-enriched EBB theories is straightforward and will be explained in passing. Conversely, the formulation of gradient-enriched TB theory has been subject to some debate on certain assumptions. First, the effects of rotational inertia were ignored by some[13] but included by others.[12,14] Second, Wang and Wang argued that in TB theory no gradient enrichment should be used in the shear constitutive relation.[15] The same assumption was made in other studies of these authors[13,14] and was motivated as follows: "no nonlocal effect is injected into the shear constitutive relation because the adopted form of Eringen's nonlocal [i.e. gradient-enriched] constitutive model (…) is not valid for the z direction."[14] In contrast, Wang and Hu used shear strain gradients in the *axial* direction of the beam.[12] We follow the latter assumption as we wish to preserve the effects of axial heterogeneity for all stress components. Below, we will formulate TB theory with rotational inertia as well as axial gradient enrichment in the shear constitutive relation.

Throughout, we will use an xy-coordinate system whereby the x-axis is aligned with the beam axis. Sign conventions for the bending moment M and the shear force Q follow from the standard sign conventions for the stresses via

$$M=\int_A y\sigma dA \tag{7}$$

and

$$Q=\int_A \tau dA = A\beta\tau \tag{8}$$

where $\sigma\equiv\sigma_{xx}$ and $\tau\equiv\sigma_{xy}$. Typical beam bending parameters are the cross sectional area A, second moment of area I, shear modulus G and shape factor β that accounts for shear in the TB theory. For thin-walled circular cross sections $A=2\pi Rt$ and $I=\pi R^3 t$ where R and t are the tube radius and wall thickness, respectively. We will also use the elastic bar velocity $c_e=\sqrt{E/\rho}$ to normalize the results where appropriate.

B. EBB theory with stress gradients

The axial equivalent of Eq. (3) reads as

$$\sigma-\ell^2\sigma_{,xx}=E\varepsilon \tag{9}$$

where ε is the axial normal strain. With Eq. (7) we obtain

$$M-\ell^2 M_{,xx}=\int_A zE\varepsilon dA = -EIw_{,xx}. \tag{10}$$

From the standard equation of motion

$$\rho A\ddot{w}=M_{,xx} \tag{11}$$

we can derive that

$$\rho A(\ddot{w}-\ell^2\ddot{w}_{,xx})=M_{,xx}-\ell^2 M_{,xxxx}=-EIw_{,xxxx}. \tag{12}$$

We use a general solution $w(x,t)=\hat{w}\exp[\mathrm{i}k(x-ct)]$ where $\hat{w}$ is the amplitude, k is the wave number and c is the phase velocity. Substituting this general solution into Eq. (12) yields

$$\frac{c^2}{c_e^2}=\frac{Ik^2}{A}\frac{1}{1+\ell^2k^2}. \tag{13}$$

C. EBB theory with strain gradients and inertia gradients

The axial stress underlying Eq. (6) is written as

$$\sigma=E(\varepsilon-\ell_s^2\varepsilon_{,xx})+\rho\ell_m^2\ddot{\varepsilon} \tag{14}$$

by which

$$M=-EI(w_{,xx}-\ell_s^2 w_{,xxxx})-\rho I\ell_m^2\ddot{w}_{,xx} \tag{15}$$

and the equation of motion is found as

$$\rho A\ddot{w}=M_{,xx}=-EI(w_{,xxxx}-\ell_s^2 w_{,xxxxxx})-\rho I\ell_m^2\ddot{w}_{,xxxx}. \tag{16}$$

Substituting $w(x,t)=\hat{w}\exp(\mathrm{i}k(x-ct))$ into Eq. (16) then results in

$$\frac{c^2}{c_e^2}=\frac{Ik^2}{A}\frac{1+\ell_s^2k^2}{1+\frac{Ik^2}{A}\ell_m^2k^2}. \tag{17}$$

D. TB theory with stress gradients

For reasons explained in Sec. III A we will not only adopt Eq. (9) but also its counterpart in shear, that is,

$$\tau-\ell^2\tau_{,xx}=G\gamma \tag{18}$$

where $\gamma\equiv\gamma_{xy}$ is the shear strain. The rotation of the cross section ϕ is related to the slope of the deflection $w_{,x}$ and the shear deformation γ as $\phi=-\gamma+w_{,x}$. We can therefore write

$$M-\ell^2 M_{,xx}=-EI\phi_{,x} \tag{19}$$

and

$$Q-\ell^2 Q_{,xx}=GA\beta(w_{,x}-\phi). \tag{20}$$

From the standard equation of motion $\rho A\ddot{w}=Q_{,x}$ we obtain

$$\rho A(\ddot{w}-\ell^2\ddot{w}_{,xx})=Q_{,x}-\ell^2 Q_{,xxx}=GA\beta(w_{,xx}-\phi_{,x}) \tag{21}$$

whereas the rotational equation of motion $\rho I\ddot{\phi}=Q-M_{,x}$ yields

$$\begin{aligned}\rho I(\ddot{\phi}-\ell^2\ddot{\phi}_{,xx})&=Q-\ell^2 Q_{,xx}-M_{,x}+\ell^2 M_{,xxx}\\&=GA\beta(w_{,x}-\phi)+EI\phi_{,xx}.\end{aligned} \tag{22}$$

The substitution of $w(x,t)=\hat{w}\exp[\mathrm{i}k(x-ct)]$ and $\phi(x,t)=\hat{\phi}\exp[\mathrm{i}k(x-ct)]$ renders

$$[c^2k^2\rho A(1+\ell^2k^2)-GA\beta k^2]\hat{w}=\mathrm{i}kGA\beta\hat{\phi} \tag{23}$$

and

$$[c^2k^2\rho I(1+\ell^2k^2) - GA\beta - EIk^2]\mathrm{i}k\hat{\phi} = GA\beta k^2\hat{w} \quad (24)$$

which, after elimination of $\hat{w}$ and $\hat{\phi}$, yields

$$\frac{c^4}{c_e^4} - \frac{c^2}{c_e^2}\frac{a_1/k^2+a_2+1}{1+\ell^2k^2} + \frac{a_2}{(1+\ell^2k^2)^2} = 0 \quad (25)$$

where $a_1 = GA\beta/EI = \beta/(1+\nu)R^2$ and $a_2 = G\beta/E = \beta/2(1+\nu)$. The solution in terms of c^2 reads as

$$\frac{c^2}{c_e^2} = \frac{a_1/k^2+a_2+1 \pm \sqrt{(a_1/k^2+a_2+1)^2-4a_2}}{2(1+\ell^2k^2)}. \quad (26)$$

Note that this result differs somewhat from the result reported by Wang,[13] since the latter study ignores rotational inertia and gradient enrichment of the shear constitutive relation.

E. TB theory with strain gradients and inertia gradients

Finally, TB theory is formulated using the gradient elasticity formulation with strain gradients and inertia gradients. We employ Eq. (14) as well as its counterpart in shear,

$$\tau = G(\gamma - \ell_s^2\gamma_{,xx}) + \rho\ell_m^2\ddot{\gamma}. \quad (27)$$

Thus,

$$M = -EI(\phi_{,x} - \ell_s^2\phi_{,xxx}) - \rho I\ell_m^2\ddot{\phi}_{,x} \quad (28)$$

and

$$Q = GA\beta(w_{,x} - \phi - \ell_s^2 w_{,xxx} + \ell_s^2\phi_{,xx}) + \rho A\beta\ell_m^2(\ddot{w}_{,x} - \ddot{\phi}). \quad (29)$$

The standard equation of motion reads as

$$\begin{aligned}\rho A\ddot{w} &= Q_{,x} \\ &= GA\beta(w_{,xx} - \phi_{,x} - \ell_s^2 w_{,xxxx} + \ell_s^2\phi_{,xxx}) \\ &\quad + \rho A\beta\ell_m^2(\ddot{w}_{,xx} - \ddot{\phi}_{,x})\end{aligned} \quad (30)$$

and the rotational equation of motion is written as

$$\begin{aligned}\rho I\ddot{\phi} &= Q - M_{,x} \\ &= GA\beta(w_{,x} - \phi - \ell_s^2 w_{,xxx} + \ell_s^2\phi_{,xx}) + \rho A\beta\ell_m^2(\ddot{w}_{,x} - \ddot{\phi}) \\ &\quad + EI(\phi_{,xx} - \phi_{,xxxx}) + \rho I\ell_m^2\ddot{\phi}_{,xx}.\end{aligned} \quad (31)$$

Simultaneous solutions $w(x,t) = \hat{w}\exp[\mathrm{i}k(x-ct)]$ and $\phi(x,t) = \hat{\phi}\exp[\mathrm{i}k(x-ct)]$ yield

$$\begin{aligned}&[c^2k^2\rho A(1+\beta\ell_m^2k^2) - GA\beta k^2(1+\ell_s^2k^2)]\hat{w} \\ &= [GA\beta(1+\ell_s^2k^2) - c^2k^2\rho A\beta\ell_m^2]\mathrm{i}k\hat{\phi}\end{aligned} \quad (32)$$

and

$$\begin{aligned}&[c^2k^2(\rho I + \rho A\beta\ell_m^2 + \rho I\ell_m^2k^2) - GA\beta(1+\ell_s^2k^2) \\ &- k^2EI(1+\ell_s^2k^2)]\mathrm{i}k\hat{\phi} = [k^2GA\beta(1+\ell_s^2) - c^2k^4\rho A\beta\ell_m^2]\hat{w}.\end{aligned} \quad (33)$$

The two amplitudes $\hat{w}$ and $\hat{\phi}$ are eliminated and after some tedious but straightforward algebra, a dimensionless quartic in terms of the phase velocity c is found as

$$\begin{aligned}&\frac{c^4}{c_e^4}\left[(1+\ell_m^2k^2)(1+\beta\ell_m^2k^2) + \frac{A}{Ik^2}\beta\ell_m^2k^2\right] \\ &- \frac{c^2}{c_e^2}\left[\frac{GA\beta}{EIk^2} + 1 + \beta\ell_m^2k^2 + \frac{G\beta}{E}(1+\ell_m^2k^2)\right](1+\ell_s^2k^2) \\ &+ \frac{G\beta}{E}(1+\ell_s^2k^2)^2 = 0,\end{aligned} \quad (34)$$

which can be solved for c^2 and, subsequently, for c.

IV. DISCUSSION OF THE WORK OF WANG AND HU (2005)

Wang and Hu[12] studied the propagation of flexural waves in CNTs. They compare molecular-dynamics simulations with several beam theories, including EBB and TB theories, as well as classical and gradient-enriched theories. In particular, they use a gradient enrichment with unstable strain gradients, see Eq. (1) in the paper by Wang and Hu.[12] Their results can be found from the results of Sec. III by taking $\ell_m^2 = 0$ and $\ell_s^2 = -\ell^2$ in the gradient elasticity theory with strain gradients and inertia gradients. Thus, for the EBB theory Wang and Hu obtain

$$\frac{c^2}{c_e^2} = \frac{Ik^2}{A}(1-\ell^2k^2) \quad (35)$$

for the phase velocity, which is a special case of Eq. (17). Similarly, for the TB theory the phase velocity is retrieved as a special case from Eq. (34), i.e.,

$$\frac{c^4}{c_e^4} - \left(\frac{a_1}{k^2} + a_2 + 1\right)(1-\ell^2k^2)\frac{c^2}{c_e^2} + a_2(1-\ell^2k^2)^2 = 0 \quad (36)$$

with again $a_1 = GA\beta/EI = \beta/(1+\nu)R^2$ and $a_2 = G\beta/E = \beta/2(1+\nu)$. This yields

$$\frac{c^2}{c_e^2} = \frac{1}{2}\left(\frac{a_1}{k^2} + a_2 + 1 \pm \sqrt{\left(\frac{a_1}{k^2} + a_2 + 1\right)^2 - 4a_2}\right)(1-\ell^2k^2), \quad (37)$$

which looks very similar to Eq. (26), the only difference being the effect of the gradient enrichment. The lower branch of Eq. (37) is of relevance for flexural waves. The discriminant in Eq. (37) can be rewritten as

$$\left(\frac{a_1}{k^2} + a_2 + 1\right)^2 - 4a_2 = (a_2-1)^2 + \left(\frac{a_1}{k^2} + 2a_2 + 2\right)\frac{a_1}{k^2}, \quad (38)$$

which is non-negative since $a_1 > 0$ and $a_2 > 0$. It then follows that the phase velocities of both Eqs. (35) and (37) are real provided that $\ell k \leq 1$. Conversely, imaginary phase velocities are found if $\ell k > 1$ for both the EBB and the TB theories. Imaginary phase velocities lead to an unbounded growth of the response in time without the need for external work, and they are therefore *destabilizing*.

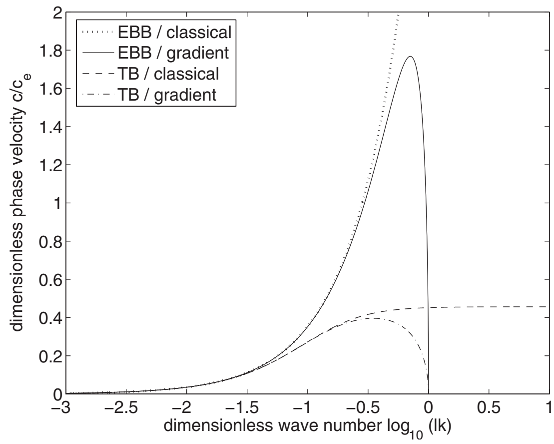

FIG. 1. Normalized phase velocity c/c_e versus logarithm of normalized wave number $\log_{10}(\ell k)$ for classical and gradient-enriched versions of EBB and TB theories according to Wang and Hu (2005).

Figure 1 shows the dispersion curves for the two beam theories in their classical and gradient-enriched variants, whereby logarithmic scaling of the horizontal axis was used to facilitate comparison with Figs. 2 and 3 in the paper by Wang and Hu.[12] These curves were obtained by assuming a ratio of tube radius R over length scale ℓ as $R/\ell=5$, a Poisson ratio $\nu=0.2$ and a shape factor $\beta=\frac{1}{2}$. A larger range of wave numbers was plotted than used in Figs. 2 and 3 of the paper by Wang and Hu,[12] which clearly reveals that both gradient-enriched theories render imaginary (hence, destabilizing) phase velocities for $\log_{10}(\ell k)>0$.

Wang and Hu compare the predictions of the four beam theories with molecular-dynamics simulations and they conclude that "the traditional [i.e. classical] Timoshenko beam is able to offer a much better prediction than the traditional Euler beam and the nonlocal [i.e. gradient-enriched] elastic Euler beam."[12] We agree that the two EBB theories are unsuitable: in classical EBB theory the phase velocity becomes unbounded for larger wave numbers, whereas in gradient-enriched EBB theory the phase velocity is imaginary (and therefore destabilizing) for larger wave numbers. We also agree that the classical TB theory is more suited than either of the two EBB theories, since in classical TB theory the phase velocities are bounded and real for all wave numbers.

Wang and Hu continued to conclude that for very large wave numbers, when the microstructure of CNTs becomes relevant, only the gradient-enriched TB theory is suitable.[12] An important criterion in this comparison is given as follows: "only the nonlocal [i.e. gradient-enriched] elastic Timoshenko beam is able to predict the *decrease of phase velocity* [our italics] when the wave number is so large that the microstructure of carbon nanotubes has a significant influence on the flexural wave dispersion."[12] We agree that certain parts of the dispersion curves may exhibit decreasing phase velocities, but we do not agree that the Timoshenko beam theory combined with unstable strain gradients is an appropriate model to capture this phenomenon. The gradient-enriched TB theory of Wang and Hu predicts imaginary (hence, destabilizing) phase velocities for wave numbers $k>1/\ell$ and is therefore not suitable. This is merely a consequence of the *type of gradient enrichment* that is chosen by Wang and Hu. In the next section, we will demonstrate that this is easily amended by adopting a stable gradient enrichment.

V. NUMERICAL RESULTS

The gradient elasticity beam theories formulated above have been used in the prediction of dispersion curves for CNTs. We have followed the work of Wang and Hu (who provide MD simulations in their paper for validation), whereby the mass density is taken as $\rho=2237\ \mathrm{kg/m^3}$. For a (5,5) armchair CNT, we set the Young's modulus $E=0.46\times10^{12}\ \mathrm{N/m^2}$ and the Poisson's ratio $\nu=0.22$, while for a (10,10) armchair CNT we set $E=0.47\times10^{12}\ \mathrm{N/m^2}$ and $\nu=0.20$. The length scale was taken as $\ell=0.0355\times10^{-9}$ m, which follows directly from the axial distance between two rings of carbon atoms;[12] this is also the value that will be adopted for ℓ_s in the model with combined strain/inertia gradients. Furthermore, in the TB theory we have taken the shear shape factor $\beta=\frac{1}{2}$, which is appropriate for thin-walled tubes.

In comparing the performance of the various models, we will adopt the following terminology: wave numbers are indicated as *small* in case $\ell k\ll1$, they are indicated as *mid-range* for $\ell k=\mathcal{O}(1)$ and as *large* for $\ell k\gg1$.

A. EBB theories

First, the performance of gradient-enriched EBB theories is studied. Figures 2 and 3 show the phase velocity versus (logarithm of) wave-number dispersion curves of the various gradient-enriched beam theories for the (5,5) armchair CNT. As a reference and in order to facilitate cross comparison between the figures, the MD simulations taken from Wang and Hu[12] are plotted as well—these MD results are only available for small and mid-range wave numbers. Note that the scale of the vertical axes in the two figures differs by more than a factor of 10. The corresponding results for the

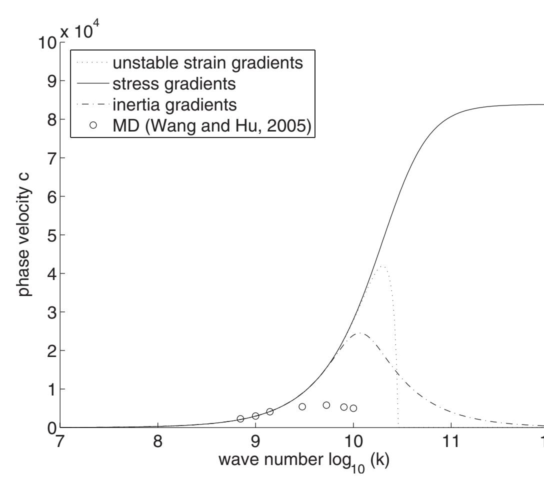

FIG. 2. Phase velocity c versus logarithm of wave number $\log_{10}(k)$ for various gradient-enriched EBB theories—(5,5) armchair CNT.

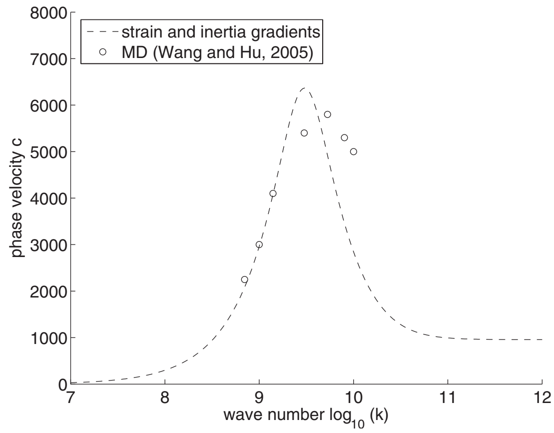

FIG. 3. Phase velocity c versus logarithm of wave number $\log_{10}(k)$ for EBB theory enriched with strain gradients and inertia gradients—(5,5) armchair CNT.

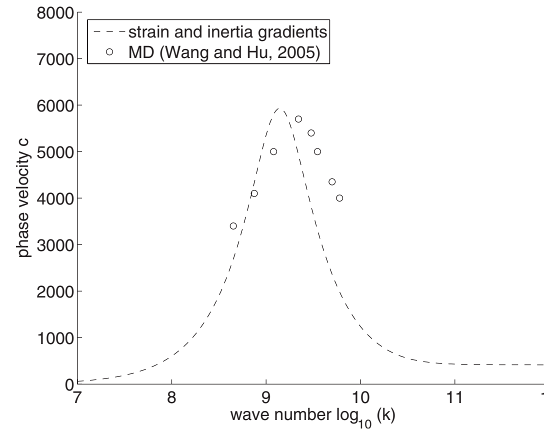

FIG. 5. Phase velocity c versus logarithm of wave number $\log_{10}(k)$ for EBB theory enriched with strain gradients and inertia gradients—(10,10) armchair CNT.

(10,10) armchair CNT are plotted in Figs. 4 and 5. The plotted results were obtained with $\ell_m/\ell_s=15$ for the (5,5) CNT and $\ell_m/\ell_s=35$ for the (10,10) CNT.

The gradient-enriched EBB theories show a wide range of predicted phase velocities. In gradient elasticity with stress gradients, the phase velocity is monotonically increasing and it attains a horizontal asymptote which is much larger than any of the values observed in the other gradient-enriched EBB models. The format with unstable strain gradients, as commented upon already in Sec. IV, predicts destabilizing phase velocities for $k>1/\ell$. The two formats with inertia gradients behave *qualitatively* the same, although there are major *quantitative* differences that are governed by the value of the inertia gradient length scale ℓ_m. Both theories predict increasing phase velocities for small-to-medium wave numbers, while the phase velocity is decreasing for medium to large wave numbers. The format with inertia gradients only (i.e., no strain gradients) approaches zero phase velocity for the larger wave numbers, whereas the format with inertia and strain gradients has a nonzero asymptote. The most important difference, however, is that the format with only inertia gradients gives results that are quite far removed from the MD simulations, whereas the format with strain gradients and inertia gradients allows a reasonable qualitative fit of the MD results for small-to-mid-range wave numbers.

The quality of this fit is of course related to the adopted value for ℓ_m. In this work, we have not carried out sophisticated curve-fitting procedures, as this would interfere with the values for the other material parameters which we have taken directly from the study of Wang and Hu.[12] However, even with such a preliminary estimate of ℓ_m, the performance of the EBB theory with strain gradients and inertia gradients is an enormous improvement over EBB theories with other types of gradient enrichment.

B. TB theories

Figures 6 and 7 show the results for the gradient-enriched TB theories. In contrast to the EBB results, the various curves obtained with gradient-enriched TB theories are much

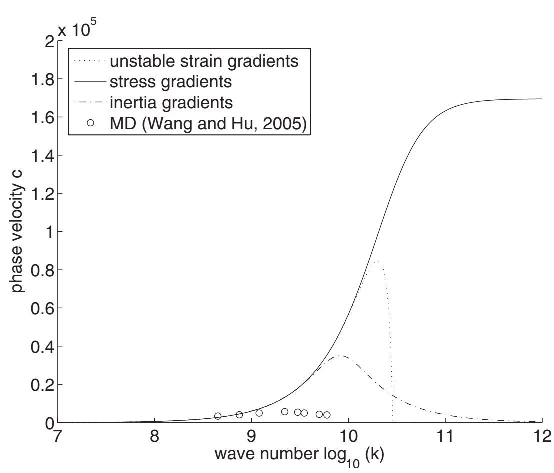

FIG. 4. Phase velocity c versus logarithm of wave number $\log_{10}(k)$ for various gradient-enriched EBB theories—(10,10) armchair CNT.

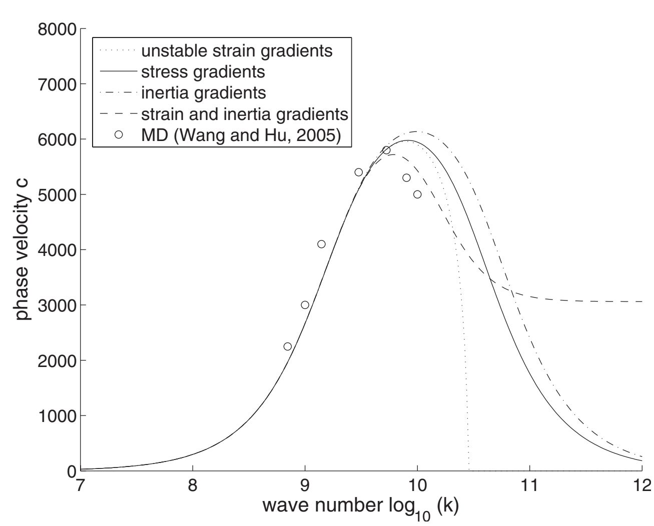

FIG. 6. Phase velocity c versus logarithm of wave number $\log_{10}(k)$ for various gradient-enriched TB theories—(5,5) armchair CNT.

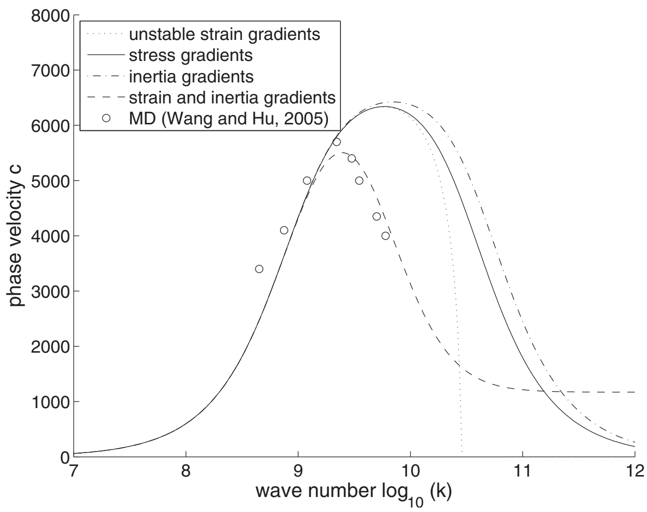

FIG. 7. Phase velocity c versus logarithm of wave number $\log_{10}(k)$ for various gradient-enriched TB theories—(10,10) armchair CNT.

closer in range. As discussed in Sec. IV, the formulation with unstable strain gradients predicts destabilizing phase velocities for $k>1/\ell$. Such instabilities are avoided altogether when stress gradients, inertia gradients, or a combination of strain gradients and inertia gradients is used. In contrast to the EBB results of Figs. 2 and 4, there is just a small deviation between the results obtained with stress gradients and inertia gradients: both are first increasing and then decreasing, they predict a maximum phase velocity for more or less the same wave number, and they predict zero phase velocities for infinitely large wave numbers. The formulation with strain gradients as well as inertia gradients differs in that a nonzero horizontal asymptote is predicted for the larger wave numbers; this asymptote is set through the parameter ℓ_m. All three stable gradient elasticity formulations (i) capture the increasing phase velocity for small-to-medium wave numbers that is predicted by MD simulations,[12] and (ii) predict a decreasing phase velocity for medium to large wave numbers, which again is in accordance with the MD simulations. However, there are some quantitative difference between the MD results and the gradient theories with stress gradients and with inertia gradients, especially for the (10,10) armchair CNT shown in Fig. 7. Conversely, with an appropriate choice for the length scale parameter ℓ_m, a good fit of the MD results can be obtained when the model with strain gradients and inertia gradients is used. The adopted values for ℓ_m are $\ell_m/\ell_s=3$ for the (5,5) CNT and $\ell_m/\ell_s=8$ for the (10,10) CNT.

The values of ℓ_m in the EBB simulations are significantly larger than the values of ℓ_m in the TB results. This may suggest that the dynamic RVE size is larger in EBB theory than in TB theory. It is, however, interesting that the value of ℓ_m seems to scale more or less linearly with the radius of the CNT, a trend which is observed both in EBB and TB theories. This observation warrants further verification and study.

VI. CONCLUSIONS

In this paper, we have discussed the dispersion of flexural waves in carbon nanotubes (CNTs). The wave dispersion due to heterogeneity of the material is modeled via gradient enrichments of the elastic continuum equations. A number of *gradient elasticity* formulations were discussed, including theories with unstable strain gradients, stable stress gradients, stable inertia gradients, or a combination of stable strain gradient and stable inertia gradients. Beam theories were formulated with the various gradient enrichments, using either the Euler-Bernoulli or the Timoshenko assumptions.

We discussed a recent study by Wang and Hu in which unstable strain gradients were employed; the resulting beam theories predict imaginary (and, hence, destabilizing) phase velocities for the larger wave numbers. Next, an overall comparison was made between the various types of gradient enrichment. Regarding the gradient-enriched Euler-Bernoulli theories, it was found that the theories with stress gradients and with inertia gradients could not provide a satisfactory prediction of the dispersive characteristics of CNTs. Reasonably accurate results, as compared to molecular-dynamics simulations, were obtained using the gradient theory with strain gradients and inertia gradients.

In contrast, Timoshenko theory in combination with either stress gradients or inertia gradients leads to results that reproduce the basic trends of the molecular-dynamics simulations reported by Wang and Hu.[12] The best results by far were obtained when Timoshenko's beam theory assumptions are coupled to gradient elasticity with combined strain/inertia gradients. This particular gradient-enriched beam theory allows for an excellent fit of the molecular-dynamics results for the entire small-to-medium range of wave numbers—it is emphasized that no MD results were available as yet for the large wave numbers.

An issue that has been discussed briefly, but not explored in detail, is the inertia-related length scale ℓ_m, which is related to the size of the material's Representative Volume Element in elastodynamics. It was found that this length scale is significantly larger in Euler-Bernoulli theory than in Timoshenko theory, and it scales with the radius of the CNT. Another issue that warrants further study is the application of gradient elasticity to CNTs of chiralities other than the armchair type, in particular the effect that this would have on the validation and/or identification of the various length scale parameters.

ACKNOWLEDGMENTS

We gratefully acknowledge financial support of the European Commission (Grant No. RTN/DEFINO HPRN-CT-2002-00198, "Deformation and fracture instabilities in novel materials and processes"). The second author also acknowledges support from the U.S. Government through NSF/NIRT Grant No. DMI-0532320, as well as the Greek Government through PENED and PYTHAGORAS programs.

*h.askes@sheffield.ac.uk
†mom@mom.gen.auth.gr

[1] C. Q. Ru, *Encyclopedia of Nanoscience and Nanotechnology* (American Scientific Publishers, Valencia, CA, 2004), pp. 731–744.
[2] K.-Y. Xu, E. C. Aifantis, and Y.-H. Yan, ASME J. Appl. Mech. **75**, 021013 (2008).
[3] K.-Y. Xu and E. C. Aifantis, "Gradient Models for Free Transverse Vibration of a Double-Walled Carbon Nanotube," Michigan Technological University, Houghton, internal report, 2008 (unpublished).
[4] E. C. Aifantis, Dislocations 2008, IOP Conf. Ser.: Mater. Sci. Eng. **3**, 012026 (2009).
[5] E. C. Aifantis, Microsyst. Technol. **15**, 109 (2009).
[6] M. Lazar, G. A. Maugin, and E. C. Aifantis, Phys. Status Solidi B **242**, 2365 (2005).
[7] M. Lazar, G. A. Maugin, and E. C. Aifantis, Int. J. Solids Struct. **43**, 1404 (2006).
[8] E. C. Aifantis, Int. J. Eng. Sci. **30**, 1279 (1992).
[9] E. C. Aifantis, ASME J. Eng. Mater. Technol. **121**, 189 (1999).
[10] E. C. Aifantis, Int. J. Fract. **95**, 299 (1999).
[11] H. Askes and E. C. Aifantis, Int. J. Fract. **117**, 347 (2002).
[12] L. Wang and H. Hu, Phys. Rev. B **71**, 195412 (2005).
[13] Q. Wang, J. Appl. Phys. **98**, 124301 (2005).
[14] C. M. Wang, Y. Y. Zhang, and X. Q. He, Nanotechnology **18**, 105401 (2007).
[15] Q. Wang and C. M. Wang, Nanotechnology **18**, 075702 (2007).
[16] W. H. Duan, C. M. Wang, and Y. Y. Zhang, J. Appl. Phys. **101**, 024305 (2007).
[17] R. D. Mindlin, Arch. Ration. Mech. Anal. **16**, 51 (1964).
[18] E. Kröner, Int. J. Solids Struct. **3**, 731 (1967).
[19] A. C. Eringen, J. Appl. Phys. **54**, 4703 (1983).
[20] S. B. Altan and E. C. Aifantis, Scr. Metall. **26**, 319 (1992).
[21] C. Q. Ru and E. C. Aifantis, Acta Mech. **101**, 59 (1993).
[22] B. S. Altan and E. C. Aifantis, J. Mech. Behav. Mater. **8**, 231 (1997).
[23] M. Yu. Gutkin and E. C. Aifantis, Scr. Mater. **35**, 1353 (1996).
[24] M. Yu. Gutkin and E. C. Aifantis, Scr. Mater. **36**, 129 (1997).
[25] A. V. Metrikine and H. Askes, Eur. J. Mech. A/Solids **21**, 555 (2002).
[26] H. Askes and E. C. Aifantis, Int. J. Fract. **139**, 297 (2006).
[27] E. C. Aifantis, J. Mech. Behav. Mater. **5**, 355 (1994).
[28] M. Yu. Gutkin and E. C. Aifantis, Scr. Mater. **40**, 559 (1999).
[29] M. Yu. Gutkin and E. C. Aifantis, *Nanostructured Films and Coatings*, NATO ASI Series (Kluwer, The Netherlands, 2000), pp. 247–254.
[30] M. Yu. Gutkin, Rev. Adv. Mater. Sci. **1**, 27 (2000).
[31] E. C. Aifantis, Mech. Mater. **35**, 259 (2003).
[32] C. Q. Ru and E. C. Aifantis, "Formulation and Solutions of Gradient Elasticity," Michigan Technological University, Houghton, internal report, 1993 (unpublished).
[33] H. Askes and A. V. Metrikine, Eur. J. Mech. A/Solids **21**, 573 (2002).
[34] H. Askes, T. Bennett, and E. C. Aifantis, Int. J. Numer. Methods Eng. **72**, 111 (2007).
[35] C. S. Chang and J. Gao, Int. J. Solids Struct. **32**, 2279 (1995).
[36] H.-B. Mühlhaus and F. Oka, Int. J. Solids Struct. **33**, 2841 (1996).
[37] H. Askes and M. A. Gutiérrez, Int. J. Numer. Methods Eng. **67**, 400 (2006).
[38] I. V. Andrianov, J. Awrejcewicz, and R. G. Barantsev, ASME Appl. Mech. Rev. **56**, 87 (2003).
[39] I. V. Andrianov and J. Awrejcewicz, Comput. Struct. **86**, 140 (2008).
[40] I. M. Gitman, H. Askes, and E. C. Aifantis, Int. J. Fract. **135**, L3 (2005).
[41] A. V. Metrikine and H. Askes, Philos. Mag. **86**, 3259 (2006).